

1
2
3
4
5
6
7
8
9
10
11
12
13
14
15
16
17
18
19
20

On the problem of tsunami run-up to a flat shore

Sergey A. Arsen'yev¹ and Lev V. Eppelbaum²

¹Institute of the Physics of the Earth, Russian Academy of Sciences, Bolshaya Gruzinskaya St., Moscow 123995, Russia

²Department of Geophysics, Faculty of Exact Sciences, Tel Aviv University, Ramat Aviv 6997801, Tel Aviv, Israel

Key points:

- A comparatively simple analytical solution to a nonlinear equation describing the tsunami run-up on a flat shore was found.
- The solution found describes a clear boundary of the front of the tsunami running ashore at a finite speed.
- Obtained solution indicates that rough shelf stops the tsunami wave by turbulence effect and it does not reach the coast

21 **Abstract**

22 When a tsunami wave comes from the ocean and propagates through the shelf, it is
23 necessary to predict the maximum flooding of the coast, the height of the tsunami on the
24 coast, the speed of the tsunami front through the coast, and other characteristics. A linear
25 solution to this problem is unsatisfactory: it gives an infinite rate of coastal flooding, that
26 is, the coast is flooded instantly and without a frontal boundary. In this study, we propose a
27 new solution in nonlinear theory to calculate these tsunami characteristics. The obtained
28 formulas show that the tsunami wave can be stopped on the shelf when approaching the
29 shore. For this, it is necessary to artificially raise several tens of bottom protrusions to the
30 level of calm water. Thus, the obtained solution allows to develop a physical-technical
31 strategy to saving human lives and preventing material damage.

32

33

34 **Plain Language Summary**

35 The problem of reducing the impact force of tsunami, and consequently the reduction in
36 the number of human casualties and the decrease of the level of destruction, is very
37 significant. However, in order to understand the interaction of the tsunami with the shelf
38 zone and the coastline, a convenient applied physical-geodynamic model of this
39 phenomenon must be created. We found that the linear model is completely unsuitable for
40 describing this complex natural phenomenon. On the basis of the many years of research
41 experience in this area, we have found a nonlinear, relatively simple, but effective model
42 of tsunami behavior near the coastline. Based on this model, a proposed solution allows to
43 stop (or considerably weaken) the effect of the impending tsunami wave.

44

45

46 Introduction

47 Tsunami are long gravitational waves in the ocean occurring as a result of a short-term
48 change in its volume, that is, due to large-scale disturbances in the ocean surface, its
49 shores, or the bottom (Arsen'yev et al., 1998; Levin and Nosov, 2016; Rabinovich, 2020).
50 Waves with a length λ exceeding the depth of the ocean H are called long waves ($\lambda > H$).
51 Therefore, tsunami cover the entire ocean's thickness (in the concrete region) and can
52 spread over transoceanic distances, that is, they are a planetary phenomenon like
53 astronomical tides. Typical tsunami wave periods are from 1 minute to several hours, and
54 characteristic wavelengths are from 1 km to 100 km. Therefore, when approaching the
55 shelf, tsunami waves can nonlinearly interact with the shallow components of the ocean
56 tide, which can weaken or strengthen the tsunami wave (Arsen'yev et al., 1993).

57 The tsunami phenomenon is a natural disaster, which has been intensively studied
58 since the second half of the 20th century. Modern tsunami studies can be tentatively
59 divided into three groups.

60 First, tsunami sources in the oceans and seas are being studied (e.g., Beisel et al.,
61 2009; Wendt et al., 2009; Allgeyer and Cummins, 2014; Lay et al., 2016). Here, the waves
62 are often calculated using the linear theory of potential, non-eddy motions of an ideal
63 frictionless fluid under the influence of gravity field (Levin and Nosov, 2016). Such
64 models are called non-hydrostatic, since they do not use shallow water equations and the
65 hydrostatic law, which are valid for the long waves. In other models, tsunami waves are
66 considered as long waves already at the source of excitement, therefore they are called as
67 hydrostatic models (Garagash and Lobkovsky, 2006; Lobkovsky et al., 2019).

68 The second group of investigators studies the propagation of tsunami waves in the
69 ocean (e.g., Beisel et al., 2009; Allgeyer, Cummins, 2014; Lay et al., 2016; Levin and
70 Nosov, 2016; Wang et al., 2017). Here the waves are considered as long ones, the
71 hydrostatic models of the theory of shallow water are used, and the process itself
72 substantially depends on the depth of the ocean (Pelinovsky, 1996).

73 In the third group of works, the process of tsunami propagation through the
74 continental shelf and coastal shallows is studied, including the process of transformation
75 and destruction of waves upon running out to the land (e.g., Carrier and Greenspan, 1958;
76 Arsen'yev, 1991; Arsen'yev et al., 1993; Didenkulova and Pelinovsky, 2000; Choi et al.,
77 2006; Namekar et al., 2009; Satake et al., 2013; Montoya and Lynett, 2018).

78 This work belongs to the third group of studies. They are the most difficult, since is
79 based on solving nonlinear equations. When a tsunami enters shallow water, nonlinear

80 accelerations become significant, the wave height increases, bottom friction intensifies,
 81 and the motion becomes very turbulent. On the other hand, the stage of tsunami landfall is
 82 the most destructive, and its study is most important from both from scientific and practical
 83 points of view.

84 The problem of tsunami approaching the shore is often solved at present with the
 85 help of the Carrier-Greenspan transformation (Carrier and Greenspan, 1958). It allows to
 86 reduce the system of nonlinear equations of hydrodynamics to a linear wave equation with
 87 respect to the wave function for a given slope of the coast α . In this paper, we solve the
 88 problem of the tsunami wave run-up over a flat plain, considering the coastal slope absent
 89 ($\alpha = 0$). The area of flooding and the range of tsunami propagation inside into the land are
 90 in this case maximal. Thus, the found solutions to the problem, are of interest for numerous
 91 experts engaged in building construction, environment and safety in the coastal zone of the
 92 oceans and seas (Arsen'yev et al., 1998; Satake et al., 2013).

93

94 **Statement of problem**

95 We choose the origin of coordinates at the sea edge of the shelf $x = 0$. The x axis is directed
 96 along the wave propagation direction perpendicular to the coast, the y axis is perpendicular
 97 to the x axis (left), the z axis is down vertically (Figures 1 and 2). The letter M denotes the
 98 width of the shelf. Let us will select the level $z = 0$ at the surface of calm water, the letter ζ
 99 denotes the wave disturbance of the sea surface, and positive value ζ is counted down from
 100 the unperturbed level of $z = 0$ (Figure 2). The letter H and r denote the average depth of the
 101 shelf and the height of the protrusions of the roughness at the bottom, respectively. Thus,
 102 the total depth of the shelf is value of $H - r$.

103 We will use the equations of shallow water theory. They are obtained from the
 104 equations of geophysical hydrodynamics by integration along the z axis in the range from
 105 $z = \zeta$ to $z = H - r$ (Arsen'yev, 1991; Røed, 2014). Assuming that there are no changes

106 along the y axis $\left(\frac{\partial}{\partial y} = 0\right)$, we write the initial equations in the form

107
$$\frac{\partial u}{\partial x} + \frac{\partial w}{\partial z} = 0, \tag{1}$$

108
$$\frac{\partial u}{\partial t} + u \frac{\partial u}{\partial x} + w \frac{\partial u}{\partial z} = g \frac{\partial \zeta}{\partial x} - \frac{1}{\rho} \frac{\partial p^a}{\partial x} - \frac{\partial R_x^z}{\partial z}. \tag{2}$$

109 Here u is the component of the flow velocity in the wave along the x axis, w is the velocity
 110 component along the z axis, p^a is the atmospheric pressure at the water surface, g is the

111 gravity acceleration, R_x^z is the vertical component of the turbulent Reynolds stresses
 112 (Reynolds, 1894), and ρ is the density of water.

113 Estimates show that when a wave comes out in shallow water, the turbulent friction
 114 $\frac{\partial R_x^z}{\partial z}$ is two to three orders of magnitude greater than the nonlinear accelerations and the
 115 non-stationary term. Therefore, the equation (2) can be written as

$$116 \quad g \frac{\partial \zeta}{\partial x} = \frac{\partial R_x^z}{\partial z} + \frac{1}{\rho} \frac{\partial p^a}{\partial x} . \quad (3)$$

117 It is necessary to add vertical boundary conditions to equations (1) and (3)

$$118 \quad z = \zeta, \quad w = \frac{\partial \zeta}{\partial t} + u \frac{\partial \zeta}{\partial x}, \quad R_x^z = R_x^0, \quad (4)$$

$$119 \quad z = H - r, \quad u = w = 0, \quad R_x^z = R_x^H. \quad (5)$$

120 Integrating equations (1) and (3) along the vertical axis from $z = \zeta$ to $z = H - r$ (it is
 121 the real depth, taking into account the protrusions of the roughness at the bottom), we
 122 obtain

$$123 \quad \frac{\partial \zeta}{\partial t} = \frac{\partial S}{\partial x}; \quad g(H - r - \zeta) \frac{\partial \zeta}{\partial x} - \left(\frac{H - r - \zeta}{\rho} \right) \frac{\partial p^a}{\partial x} = R_x^H - R_x^0, \quad (6)$$

124 and when integrating, we took into account the boundary conditions (4) and (5).

125 In equation (6), R_x^0 is the turbulent stress on the surface of the water caused by the
 126 action of the wind. This stress, as well as the atmospheric pressure gradient $\partial p^a / \partial x$,
 127 should be taken into account only when studying the processes of occurrence of storm
 128 surges and meteorological tsunamis (Arsen'yev and Shelkovnikov, 2010; Rabinovich,
 129 2020). In our case, when studying the tsunami wave approach to the shore, these terms can
 130 be neglected. We associate the water turbulent friction on the bottom R_x^H with the total
 131 flow S by a linear law

$$132 \quad R_x^H = \omega_T S, \quad \omega_T = \frac{3A}{(H - r)^2}, \quad S = \int_{\zeta}^{H - r} u dz. \quad (7)$$

133 Here ω_T is the friction frequency, and A is the shear vertical turbulent viscosity
 134 coefficient (Arsen'yev and Shelkovnikov, 2010).

135 Thus, equations (6) can be written as

136
$$\frac{\partial \zeta}{\partial t} = \frac{\partial S}{\partial x}; \quad g(H-r-\zeta) \frac{\partial \zeta}{\partial x} = \omega_T S. \tag{8}$$

137 Two equations (8) can easily be reduced to one nonlinear equation of parabolic type
 138 with respect to the level ζ

139
$$\frac{\partial \zeta}{\partial t} = \frac{\partial}{\partial x} \left[K(\zeta) \frac{\partial \zeta}{\partial x} \right], \tag{9}$$

140 in which the wave diffusion coefficient

141
$$K(\zeta) = \frac{g(H-r)}{\omega_T} - \left(\frac{g}{\omega_T} \right) \zeta \tag{10}$$

142 depends on an unknown quantity ζ .

143 Similar equations were studied in static physics (Boltzmann, 2011), in the theory of
 144 filtration (Boussinesq, 1904; Polubarinova-Kochina, 1971; Barenblatt, 1996), in the theory
 145 of atomic explosions (Zeldovich and Companaetz, 1950; Tikhonov and Samarskiy, 1963),
 146 in biomedical engineering (Kardashov et al., 1999; 2000), and in the theory of tornadoes
 147 (Arsen'yev et al., 2010). To solve them, numerical methods (Tikhonov and Samarskiy,
 148 1963) and approximate analytical methods (Zeldovich and Companaetz, 1950;
 149 Polubarinova-Kochina, 1971; Barenblatt, 1996) have been developed. In this paper, we
 150 propose an elegant automodel solution to the problem, which describes the phenomenon
 151 under study with sufficient for practice accuracy.

152

153 **Task solution**

154 We first consider the simple case of a deep shelf, when $H-r \gg \zeta$. Then equation (9) can
 155 be written as

156
$$\frac{\partial \zeta}{\partial t} = K_L \frac{\partial^2 \zeta}{\partial x^2}. \tag{11}$$

157 This is a classical parabolic equation of the type of the diffusion equation (or heat
 158 conduction) (Eppelbaum et al., 2014), which describes the process of tsunami wave
 159 dissipation on the shelf. It has the character of turbulent spreading with a diffusion
 160 coefficient

161
$$K_L = \frac{g H (1-n)}{\omega_T} = \frac{g H^3 (1-n)^3}{3 A} . \tag{12}$$

162 Here $n = r/H$ is the relative roughness of the ocean bottom. This process can be
 163 understood by solving equation (11) with corresponding initial (13) and boundary
 164 conditions (14):

165
$$\text{by } t \leq 0, \quad \zeta = 0 \quad \text{for all } x, \tag{13}$$

166
$$\text{by } t > 0, \quad \zeta = \zeta_0; \text{ by } x = 0, \quad \zeta = 0 \quad \text{by } x \rightarrow \infty. \tag{14}$$

167 As a result, we will be able to determine the horizontal emission of the tsunami wave
 168 to the shore, that is, the maximum range of tsunami propagation inland. We have

169
$$\zeta = \zeta_0 \left[1 - \Phi \left(\frac{x}{2 \sqrt{K_L t}} \right) \right], \tag{15}$$

170 where

171
$$\Phi \left(\frac{x}{2 \sqrt{K_L t}} \right) = \frac{2}{\sqrt{\pi}} \int_0^{\mu} \exp(-\eta^2) d\eta \tag{16}$$

172 is the probability integral in which the upper limit $\mu = \frac{x}{[2(K_L t)^{1/2}]}$.

173 The thickness of the coastal strip flooded by the tsunami wave, i.e., a surge δ , can be
 174 found from the condition of a sufficiently noticeable decrease in the level ζ when moving
 175 away from the beginning $x = 0$

176
$$\zeta = \zeta_0 \operatorname{erfc} \left(\frac{\delta}{2 \sqrt{K_L t}} \right) = 0.01 \zeta_0, \tag{17}$$

177 where

178
$$\operatorname{erfc} \left(\frac{x}{2 \sqrt{K_L t}} \right) = 1 - \Phi \left(\frac{x}{2 \sqrt{K_L t}} \right) \tag{18}$$

179 is the additional probability integral.

180 The numerical value 0.01 is reached by the *erfc* function when the value of its
 181 argument $x [4 K_L t]^{-1/2}$ is equal to two. Hence

182
$$\delta = 4 \sqrt{K_L t} = 4 \sqrt{\frac{g H (1-n) t}{\omega_T}}, \tag{19}$$

183 or

184
$$\delta = 4 \sqrt{\frac{g H^3 (1-n)^3 t}{3A}}. \tag{20}$$

185 It follows from equation (20) that the width of the flood zone δ does not depend on
 186 the amplitude of the tsunami wave ζ_0 falling to the shelf zone, does not depend on the
 187 width of the shelf M , but very strongly depends on the depth of the shelf H , the relative
 188 roughness $n = \frac{r}{H}$ and time t of tsunami action. Process of turbulence destroys the tsunami
 189 wave, therefore, with an increase in the shear turbulent viscosity coefficient A , the width of
 190 the flood zone δ decreases.

191 For $A = 10 \text{ m}^2/\text{s}$, $n = 0$ (smooth bottom) and $H = 10 \text{ m}$, from formula (20) follows
 192 that for $t = 1 \text{ hour}$, $\delta = 4300 \text{ m}$. With a shelf width of $M = 2000 \text{ m}$, the coast will be
 193 flooded by 2300 m. However, with a very rough bottom (reefs, rocky ledges at the bottom)
 194 when $n = 0.5$, we have (for the same depth, time and turbulent viscosity) from formula (20)
 195 $\delta = 1500 \text{ m}$, i.e. a wave the tsunami completely attenuates on the shelf with a width of $M =$
 196 2000 m . We see that the tsunami attack can be stopped by creating flood barriers or berms
 197 on the shelf with a height of $r = H$. In this case, $n = 1.1 - n = 0$ and from formula (12)
 198 follows that $K_L = 0$. Equation (16) gives

199
$$\frac{2}{\sqrt{\pi}} \int_0^\infty \exp(-\eta^2) d\eta = 1 \tag{21}$$

200 and from solution of equation (15) we get $\zeta = 0$. Thus, the tsunami run-up stops on the
 201 shelf, and the coast remains dry (intact).

202 Note that the obtained solution is approximate and has two fundamental
 203 disadvantages. First, the width of the flood zone, strictly speaking, is infinite. And we cut it
 204 off artificially, using condition (17). Secondly, water spreads through the shelf and shore
 205 with infinite speed, which is unrealistic one. These shortcomings belong to any solution of
 206 a degenerate linear parabolic equation (11). However, as we will see now, they are absent
 207 in the solution of the nonlinear equation (9).

208 Let us introduce the length scale $h = H - r$, time scale $T = h^2/A$, dimensionless
 209 coordinate $\varphi = x/h$ and dimensionless time $\tau = t/T$. Then the dimensionless diffusion
 210 coefficient

211
$$\Lambda = \frac{K}{A} = \frac{g h^3 (1-e)}{3A^2} = G \mathcal{G}, \tag{22}$$

212 where $e = \zeta/h$ is the dimensionless level disturbance, $G = \frac{gh^3}{3A^2}$ is some parameter (the
 213 authors of the paper suggest to call it as 'Galileo's number'), and $\theta = 1 - e$ is the relative
 214 water surface level.

215 Then equation (9) takes the form

$$216 \quad \frac{\partial \mathcal{G}}{\partial \varphi} = G \frac{\partial}{\partial \varphi} \left(\mathcal{G} \frac{\partial \mathcal{G}}{\partial \varphi} \right). \quad (23)$$

217 Its solution

$$218 \quad \mathcal{G}(\varphi, \tau) = \mathcal{G}_0 \tau \left(1 - \frac{\varphi}{c\tau} \right) \quad \text{by } \varphi < c\tau, \quad (24)$$

$$219 \quad \mathcal{G}(\varphi, \tau) = 0 \quad \text{by } \varphi \geq c\tau. \quad (25)$$

220 It is easy to verify that it satisfies not only equation (23), but the boundary condition
 221 at the beginning of coordinates $x = 0$, $\varphi = 0$ and the initial condition $\tau = t = 0$:

$$222 \quad \mathcal{G}(0, \tau) = \mathcal{G}_0 \tau, \quad \mathcal{G}(\varphi, 0) = 0. \quad (26)$$

223 Here θ_0 is the initial constant value. For example, for $\theta_0 = 1$, we have $\zeta_0 = 0$, i.e., there is
 224 no initial perturbation of the water surface level.

225 Indeed, substituting the solution (24) into equation (23), we obtain $c = (G \theta_0)^{1/2}$
 226 and

$$227 \quad c = \frac{h}{A} \sqrt{\frac{g(h - \zeta_0)}{3}}. \quad (27)$$

228 The coordinates of the moving point x^* of the water edge, that is the nose of the
 229 tsunami wave running onto the shore (where $\theta = 1, \zeta = 0$), is determined from the equation

$$230 \quad 1 = \mathcal{G}_0 \tau \left(1 - \frac{\varphi^*}{c\tau} \right), \quad (28)$$

231 which is equivalent to the equation

$$232 \quad \varphi^* = c\tau - \frac{c}{\mathcal{G}_0}. \quad (29)$$

233 From this follows that $c = \frac{d\varphi^*}{d\tau} = \frac{T}{h} \frac{dx^*}{dt}$, or in dimensional form

234

$$235 \quad V = \frac{dx^*}{dt} = \left(\frac{h}{T}\right)c = \sqrt{\frac{g(H-r-\zeta_0)}{3}}. \quad (30)$$

236 Tsunami nose coordinate (water edge) $x^* = \delta_n$ moves according to the law

$$237 \quad x^* = \left(t - \frac{h^2}{A g_0}\right) \sqrt{\frac{g(H-r-\zeta_0)}{3}}. \quad (31)$$

238 **Discussion**

239 Solutions (24) - (30) describe simple, but actual physical-geodynamical model of tsunami
 240 wave running onto a coastal plain with a finite velocity of (30). It differs from the
 241 Lagrange velocity $(gH)^{1/2}$ of long waves, since roughness r , initial perturbation of the
 242 water level ζ_0 and turbulent friction are taken into account here. It can be seen from
 243 formula (27) that a tsunami wave with $\zeta_0 = 0$ can be eliminated by creating roughness
 244 protrusions with a height of $r = H$, $h = 0$ at the bottom of the shelf. However, in contrast
 245 to the linear case, the tsunami wave is not just scattered over the shelf, but stops (or greatly
 246 weaken) because equation (30) indicates that its speed V vanishes.

247 Figure 3 shows the dependence of the total depth $D = H - z_0 - \zeta$ on the distance x
 248 for three time instants. Let us we stand on the shore of a beach with a width of $M = 300$ m
 249 near the water edge at a point $x = 300$ m from the beginning of coordinates, which is
 250 located on the sea edge of this beach (Fig. 1). Then the wave will begin to cover us,
 251 starting at the time $t = 166$ s, after the arrival of the wave from the origin $x = 0$. At time $t =$
 252 387 s, the wave will lift us to a height of 2.21 m, and at time $t = 664$ s – to a height of 5 m.
 253 If after that, the flow of water to the origin ceases, $\theta(x=0; \tau > 664s) = 1$, then the water
 254 that flooded the coastal plain on it will remain until the evaporation and infiltration into the
 255 soil will drain this coast.

256 The calculations shown in Fig. 3 are done for $\theta_0 = 1$, $\zeta_0 = 0$, depth $h = 1$ m and
 257 velocity $V = 1.8$ m/s. Analyzing Fig. 3, we see that the region covered by the tsunami
 258 $\partial_n = x^*$ is finite and moves at a speed V described in equation (30). Let us compare the
 259 size of the flood zone δ according to linear δ and nonlinear theory δ_n , setting $H = 10$ m, θ_0
 260 $= 1$, $\zeta_0 = 0$ and $r = 0$ (smooth bottom). According to the aforementioned nonlinear (more
 261 exact) theory, $V = 5.71$ m/s, and for 1 hour tsunami will flood an area of size $\delta_n = 20,500$

262 m. The linear theory presented in equation (20) gives for $A = 10 \text{ m}^2/\text{s}$ the size of $\delta = 4,300$
 263 m, that is 4.7 times smaller.

264 For a very rough bottom, when $H = 10 \text{ m}$, $r = 5 \text{ m}$, $h = 5 \text{ m}$, $n = 0.5$, we have $V = 4$
 265 m/s and the nonlinear theory gives $\delta_n = 14,500 \text{ m}$. The linear theory at $A = 10 \text{ m}^2/\text{s}$ gives in
 266 this case $\delta = 1,530 \text{ m}$, that is 9.4 times less. As you can see, the linear approximation gives
 267 great errors. The fact is that the diffusion coefficient K in the equation (9) stands near the
 268 highest derivative. Therefore, the solutions of this equation substantially depend on the
 269 value of $K(\zeta)$.

270 The solution of equation (24) also makes it easy to reconstruct the dependence of
 271 the depth D and the average flow velocity $U = S/h$ on time t at various fixed distances x
 272 from the source. Corresponding nomograms and graphs can be used for engineering
 273 assessments in the construction of structures that will protect especially important objects
 274 (for example, nuclear and thermal power plants, chemical plants, airfields and others
 275 (Arsen'yev et al., 1998)) located nearly the shores of the seas and oceans from the tsunami
 276 phenomenon.

277

278 **Conclusions**

279 Let us state the main results obtained in this paper. Based on the nonlinear theory of
 280 shallow water, taking into account turbulent friction on a rough bottom, the theory of
 281 tsunami roll-up to a flat shore is constructed. Exact solutions of linearized and nonlinear
 282 equations are found. It is shown that the use of solutions of linearized equations leads to
 283 large errors. The obtained formulas make it easy to calculate the advancement of the water
 284 front inland, the height of flooding of the shelf and shore at a given point, the tsunami
 285 wave propagation range, the average current velocity in the wave, and other characteristics
 286 necessary for engineering calculations. It was established that the speed of the tsunami
 287 wave can be turned to zero, that is, the movement of the tsunami wave can be stopped
 288 when approaching the coast, on the shelf. To realize this, it is necessary to increase the
 289 height of the roughness protrusions (possibly using artificial adjustable structures) on the
 290 bottom of the shelf r to the level of undisturbed depth of the shelf H . The strong turbulent
 291 friction about the bottom that occurs destroys the tsunami wave on the shelf and the
 292 tsunami wave does not reach the shore.

293

294

295 **Acknowledgements**

296 We acknowledge The Institute of the Physics of the Earth (Moscow) and Faculty of Earth
297 Sciences of Tel Aviv University for supporting this investigation. Our paper is analytical
298 and we do not use here any observed geophysical data.

299

300 **References**

- 301 Allgeyer, S., and P. Cummins (2014), Numerical tsunami simulation including elastic loading
 302 and sea water density stratification, *Geophysical Research Letters*, *41*, 2308-2375,
 303 <https://doi.org/10.1002/2014GL059348>.
- 304 Arsen'yev, S.A. (1991), On the nonlinear equations of long sea waves, *Water Resources*,
 305 No.1, 29-35 (in Russian).
- 306 Arsen'yev, S.A., V.A. Babkin, A.Yu. Gubar, and V.N. Nikolaevskiy (2010), *Theory of*
 307 *Mesoscale Turbulence. Eddies of the Atmosphere and the Ocean. Regular and Chaotic*
 308 *Dynamics*, Inst. of Computer Sciences, Moscow-Izhevsk, 2010 (in Russian).
- 309 Arsen'yev, S.A., L.N. Rykunov, and N.K. Shelkovnikov (1993), Nonlinear interactions of
 310 tsunami and tides in an ocean, *Doklady of Russian Acad. of Sci.*, *331*, No. 6, 732-734.
- 311 Arsen'yev, S.A., and N.K. Shelkovnikov (2010), Storm Surges as Dissipative Solitons.
 312 *Moscow Univ. Physics Bull.*, *68*, No. 6, 483-489.
- 313 Arsen'yev, S.A., O.A. Zhivogina, S.V. Seleverstov, and N.K. Shelkovnikov (1998), Power
 314 influence of tsunami waves on the nuclear station, *Atomic Energy*, *85*, No. 1, 69-72 (in
 315 Russian).
- 316 Barenblatt, G.I. (1996), *Scaling, Self-Similarity, and Intermediate Asymptotic*, Cambridge
 317 Univ. Press, Cambridge.
- 318 Beisel, S., L. Chubarov, I. Didenkulova, E. Kil, A. Levin, E. Pelinovsky, Y. Shokin, and M.
 319 Sladkevich (2009), The 1956 Greek tsunami recorded at Yafo, Israel, and its numerical
 320 modeling. *Journal of Geophysical Research*, *114*, CO 9092, 1-18,
 321 <https://doi.org/10.1029/2008JC005262>.
- 322 Boltzmann, L. (2011), *Lectures on Gas Theory*, Dover Publ., Inc. NY, USA.
- 323 Boussinesq, J. (1904), Recherches theoriques sur L'ecoulement des nappes d'eau infiltrées
 324 dans le sol, *Jour. de math. pures et appl.*, *Ser. 5, t. X*, fasc.1.
- 325 Carrier, G. F., and Greenspan H. P. (1958), Water waves of finite amplitude on a sloping
 326 beach, *Journal of Fluid Mechanics*, *4*, 97-109.
- 327 Choi, B.H., S.I. Hong, and E. Pelinovsky (2006), Distribution of run up heights of the
 328 December 26, 2004 tsunami in the Indian Ocean, *Geophysical Research Letters*, *33*,
 329 L13601, 1-4, doi: 10.1029/2006GL025867.
- 330 Didenkulova, I., and E. Pelinovsky (2020), Tsunami run-up on a plane beach in a tidal
 331 environment, *Pure and Applied Geophysics*, *177*, 1583-1593, [doi.org/10.1007/s00024-](https://doi.org/10.1007/s00024-019-02332-y)
 332 [019-02332-y](https://doi.org/10.1007/s00024-019-02332-y)
- 333 Eppelbaum, L.V., I.M. Kutasov, and A.N. Pilchin (2014), *Applied Geothermics*, Springer,
 334 Heidelberg – N.Y.
- 335 Garagash, L.A. and L.I. Lobkovsky (2006), An analysis of the dynamic displacement process
 336 of the sea bottom due to a subduction zone earthquake, *Trans. of the 4th Int. FLAC*
 337 *Symposium on Numerical Modelling in Geomechanics* (H. Varona, Ed.), Paper 06-01.
 338 Itaca Consulting Groups. Inc. Minneapolis, USA, 1-5.

- 339 Kardashov, V.R., S. Einav, L.V. Eppelbaum, and A. Ismail-Zadeh (1999), Novel approach to
 340 investigation and control of nonlinear nonstationary processes: application to
 341 environments and biomedical engineering, *Scientific Israel*, No.3, 24-33.
- 342 Kardashov, V.R., L.V. Eppelbaum, and O.V. Vasilyev (2000), The role of nonlinear source
 343 terms in geophysics, *Geophysical Research Letters*, 27, No.14, 2069-2072,
 344 <https://doi.org/10.1029/1999GL011192>
- 345 Lay, T., L. Li, and K.F. Cheung (2016), Modelling tsunami observations to evaluate a
 346 proposed late tsunami earthquake stage for the 16 September 2015 Illapel, Chile, Mw 8.3
 347 earthquake, *Geophysical Research Letters*, 43, 7902-7912, doi: 10.1029/2006GL025867.
- 348 Levin, B.W., and M.A. Nosov (2016), *Physics of Tsunami*, Springer, AG Switzerland.
- 349 Lobkovsky, L.I., I.A. Garagash, and R.Kh. Mazova (2019), Numerical simulation of tsunami
 350 waves generated by the underwater landslide for the Northern Coast of the Black Sea
 351 (Dzhubga Area), *Geophysical Jour. International*, 218, 1298–1306, doi:
 352 10.1093/gji/ggz221
- 353 Montoya, L., and P. Lynett (2018), Tsunami versus infragravity surge: Comparison of the
 354 physical character of extreme run up, *Geophysical Research Letters*, 45, 12,982-12,990,
 355 doi: 10.1029/2018GL080594
- 356 Namekar, S., Y. Yamasaki, and K.C. Cheung (2009), Neural network for tsunami and run up
 357 forecast, *Geophysical Research Letters*, 36, L08604, 1-6, doi:10.1029/2009GL037184
- 358 Pelinovsky, E.N. (1990), *Hydrodynamics of Tsunami Waves*, Inst. of Applied Physics of the
 359 Russ. Acad. of Sci., Nizhny Novgorod, Russia (in Russian).
- 360 Polubarinova-Kochina, P.Ya. (1971), *Theory of Ground Water Movement*, Nauka, Moscow
 361 (in Russian).
- 362 Rabinovich, A.B. (2020), Twenty-seven years of progress in the science of meteorological
 363 tsunami following the 1992 Daytona Beach events, *Pure and Applied Geophysics*, 177,
 364 1193-1230, doi.org/10.1007/s00024-019-02349-3
- 365 Reynolds, O. (1894), On the dynamical theory of incompressible viscous fluids and the
 366 determination of the criterion, *Philosoph. Trans. Royal Soc.*, London, 186, 123-161.
- 367 Røed, L.P. (2014), *Fundamentals of Atmospheres and Oceans on Computers*, University of
 368 Oslo, Institute of Geosciences.
- 369 Satake, K., Y. Fujii, T. Harada, and Y. Namegaya (2013), Time and space distribution of
 370 coseismic slip of the 2011 Tohoku earthquake as inferred from tsunami waveform data,
 371 *Bull. of Seismological Society of America*, 103, No. 2B, 1165-1170,
 372 <https://doi.org/10.1785/0120120122>
- 373 Tikhonov, A.N., and A.A. Samarsky (1963), *Equations of Mathematical Physics*, Pergamon
 374 Press, Oxford.
- 375 Wang, Y., K. Satake, T. Maeda, and A.B. Gusman (2017), Green's function - based tsunami
 376 data assimilation: A fast data assimilation approach toward tsunami early warning,
 377 *Geophysical Research Letters*, 44, 10,282-10,289, doi:10.1002/2017GL075307
- 378 Wendt, J., D.D. Oglesby, and E.L. Geist (2009), Tsunami and splay fault dynamics,
 379 *Geophysical Research Letters*, 36, L15303, 1-5, doi: 10.1029/2009GL038295

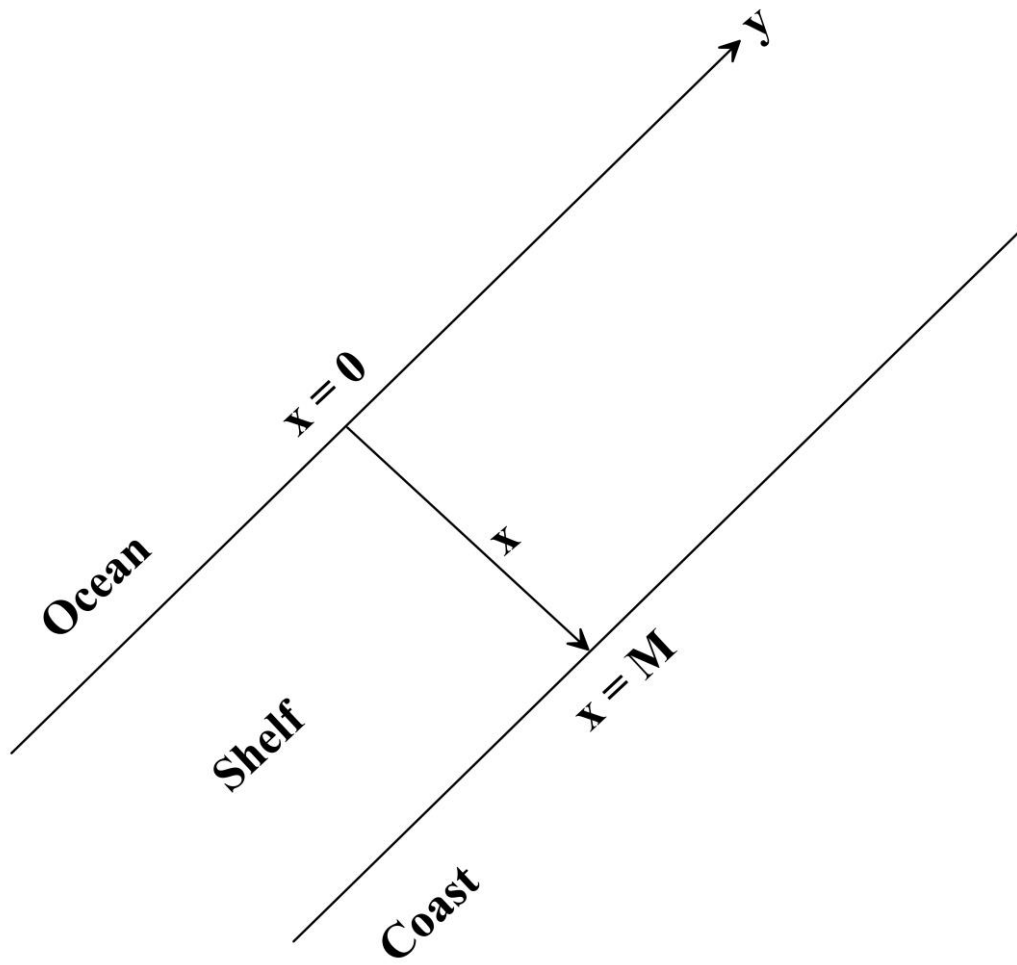
380 Zeldovich, Ya.B., and A.S. Compaetz (1950), On the theory of heat propagation with
381 temperature-depended thermal conductivity, *Coll. of papers dedicated to the 70th*
382 *anniver. of Academician A.F. Ioffe*. USSR Acad. of Sci., Moscow, 61-71 (in Russian).

383

384

385

386

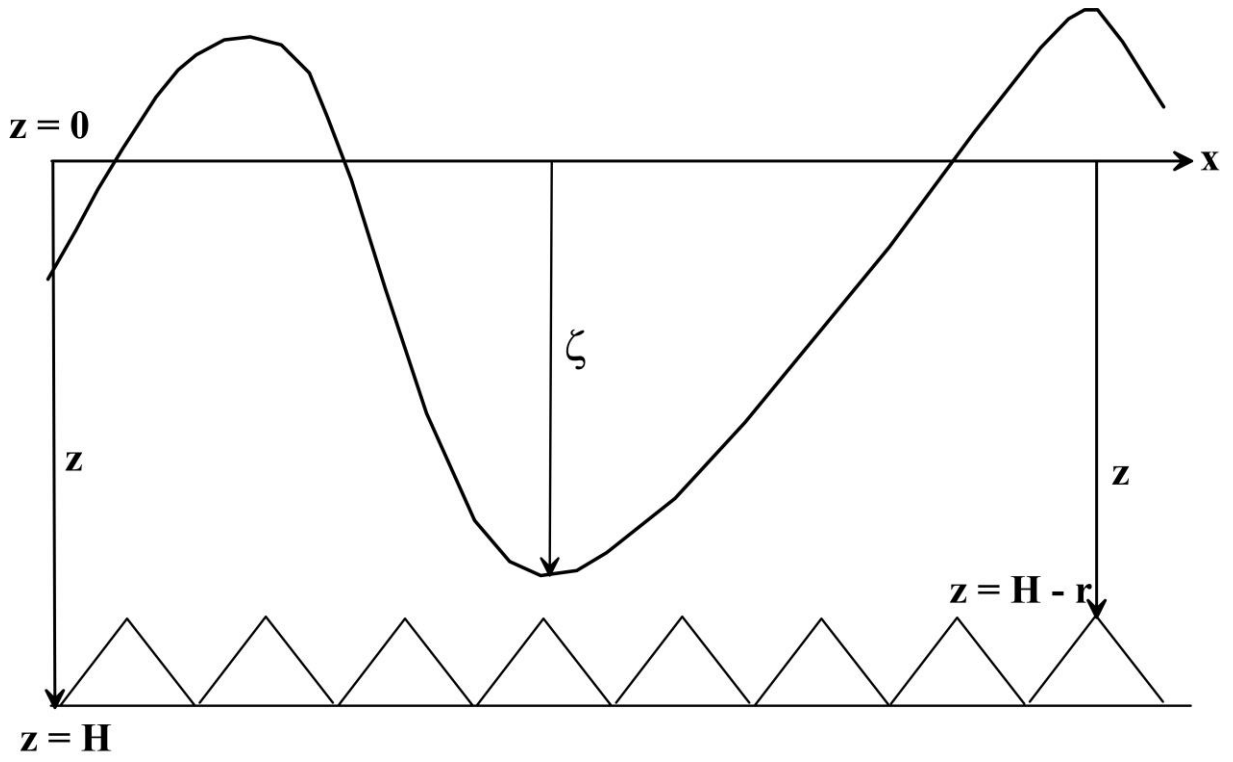


387

388 **Figure 1.** Horizontal coordinate axes and designations

389

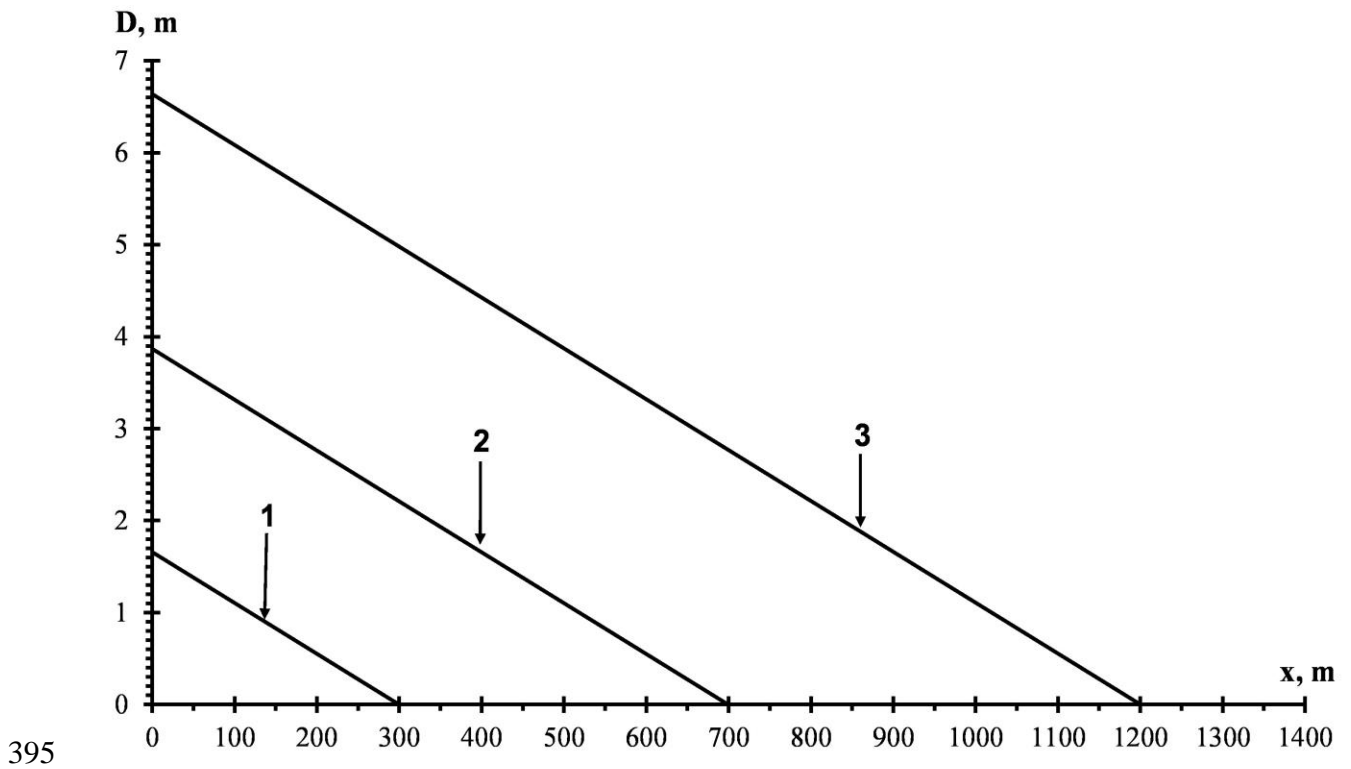
390



391
392

393 **Figure 2.** Vertical section of the water flow and corresponding designations

394



396 **Figure 3.** Dependence of the total depth of water flow D on the distance x at various time
 397 intervals. Graph 1 – $t = 166$ s, water edge is located at $x = 300$ m. Graph 2 – $t = 387$ s,
 398 water edge is located at $x = 700$ m. Graph 3 – $t = 664$ s, water edge is located at $x = 1200$
 399 m.

400